Journal of ELECTRONIC MATERIALS, Vol. 37, No. 3, 2008
DOI: 10.1007/s11664-007-0344-9

Regular Issue Paper

Interfacial Reaction Between Cu Substrates and Zn-Al Base High-Temperature Pb-Free Solders

YOSHIKAZU TAKAKU,[1,4] LAZUARDI FELICIA,[2] IKUO OHNUMA,[1] RYOSUKE KAINUMA,[3] and KIYOHITO ISHIDA[1]

1.—CREST-JST, Department of Material Science, Tohoku University, 6-6-02 Aoba-yama, Sendai 980-8579, Japan. 2.—Department of Material Science, Tohoku University, 6-6-02 Aoba-yama, Sendai 980-8579, Japan. 3.—CREST-JST, IMRAM, Tohoku University, 2-1-1 Katahira, Sendai 980-8577, Japan. 4.—e-mail: yskz-ta@material.tohoku.ac.jp

Chemical reactions between Cu substrates and Zn-Al high-temperature solder alloys, Zn-4Al and Zn-4Al-1Cu (mass%), at temperatures ranging from 420°C to 530°C were experimentally investigated by a scanning electron microscope using backscattered electrons (SEM-BSE) and an electron probe microanalyzer (EPMA). Intermediate phases (IMPs), β(A2) or β'(B2), γ($D8_2$), and ε(A3) phases formed and grew during the soldering and aging treatments. The consumption rate of the IMP for Cu substrates is described by the square root of t in both the alloys, while the additional Cu in the molten Zn-Al alloy slightly suppresses the consumption of Cu substrates. The growth of IMPs during soldering treatment is controlled by the volume diffusion of constituent elements, and its activation energy increases in the order of $Q_\varepsilon < Q_\gamma < Q_\beta$. In view of the aging process, the growth of IMPs is considered to be controlled by the volume diffusion. In particular, the layer thickness of γ rapidly grows over 200°C, although the thickness of the β layer grows very slowly.

Key words: Cu, intermediate phases (IMP), reaction, solder

INTRODUCTION

Solder alloys possessing a relatively high melting temperature are required for step soldering treatment in power-device packages, i.e., a die attachment is initially attached to a lead frame with the high-melting-temperature solder, and then the package is connected to a printed wiring board with low-melting-temperature solder. Pb-5Sn and Pb-10Sn (mass%) solders with melting points (m.p.) of 305°C and 310°C, respectively, have been widely used because of their desirable properties such as good wettability, high ductility, low shear modulus, etc. However, recent recognition of the toxicity of Pb to the environment and human health has encouraged great effort to develop Pb-free solders.

The Au-20Sn eutectic alloy has been studied as a potential Pb-free high-temperature solder which can be substituted for conventional Pb-Sn solders.[1] Although showing satisfactory properties such as suitable melting temperature (280°C), good thermal and electrical conductivities, and good fluidity and wettability, this alloy system has some problems associated with low ductility and high cost, preventing its wide application. Recently, Zn-Al base alloys have been suggested as candidates for the Pb-free high-temperature solder.[2] Figure 1a shows the Zn-Al binary phase diagram assessed by Okamoto,[3] where there is a eutectic reaction at about 6 mass% Al with the eutectic temperature at 381°C. Although the melting temperature is higher than those of Pb-Sn high-temperature solders and the effects of alloying elements, i.e., Mg, Sn, In, Ga, and Cu, on the melting temperature, hardness, wettability, etc., have been reported for Zn-Al base alloys,[2,4] there has been no report on the chemical reaction near the interface of the Cu substrate and Zn-Al solder, where the formation and growth of some intermediate phases (IMPs) such as β(A2:

(Received July 30, 2007; accepted October 29, 2007; published online November 20, 2007)

disordered bcc) or β'(B2: ordered bcc), γ($D8_2$: Cu_5Zn_8) and ε(A3: disordered hcp) are expected from the Zn-Cu phase diagram shown in Fig. 1b.[5]

In the present study, the chemical reactions occurring at the interface between a Cu substrate and Zn-4Al and Zn-4Al-1Cu (mass%) alloys during soldering and aging treatments were investigated.

EXPERIMENTAL PROCEDURE

Ingots of UNS Z35530 (AG40A: Zn-4Al mass%) and UNS Z33521 (AG41A: Zn-4Al-1Cu mass%) alloys, which are practically applied for die casting materials, were used. Solder sheets were sliced from the ingots and cut into pieces of 5 mm × 5 mm × 0.5 mm. On the other hand, the Cu plates used as dies (12 mm × 10 mm × 1 mm) and substrates (15 mm × 15 mm × 2 mm) were prepared from sheet specimens obtained by cold-rolling from an ingot of pure Cu (99.99%). After polishing with 0.3-μm alumina powder to remove the oxide layer on the surface, the Cu die, the Zn-Al base solder sheet, and the Cu substrate were stacked, placed on a hot plate that was heated to 420°C, 450°C, 500°C, and 530°C, and soldered for durations of 1 to 60 min in an Ar atmosphere to make joined assemblies.

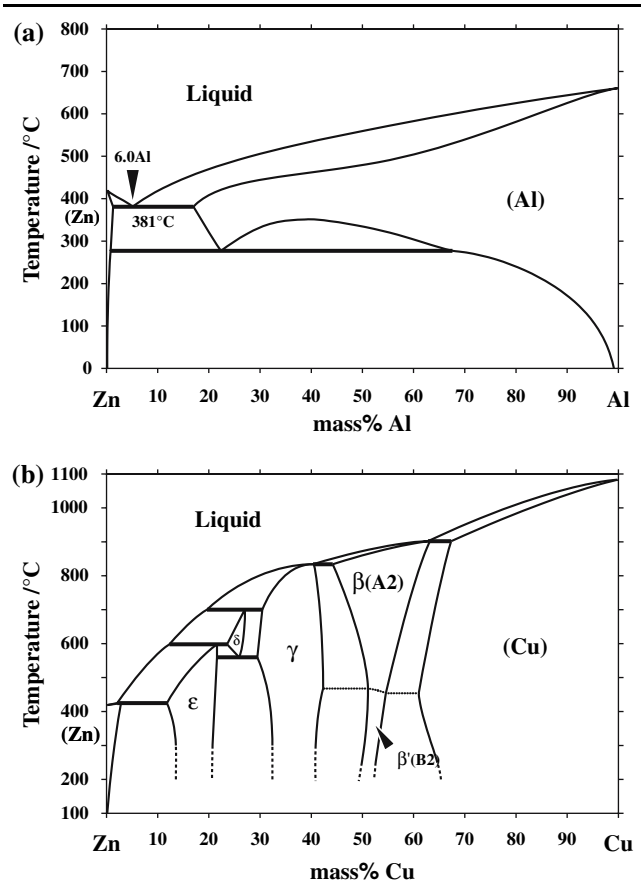

Fig. 1. Phase diagram of the (a) Zn-Al[3] and (b) Cu-Zn[5] binary systems.

An optical microscope (OM) and a scanning electron microscope (SEM: JEOL JSM-6300F) were used to observe the microstructures in the vicinity of the Cu/Zn-Al base solder interfaces. The thickness of each IMP layer formed in the diffusion zone was determined based on the average of the data obtained at five positions for each sample. The compositions of each phase in the alloy specimens and the concentration-penetration profiles in the vicinity of the interface were determined by an electron probe microanalyzer (EPMA).

The assemblies soldered at 460°C for 5 min were heated again to 120°C, 200°C, and 300°C and aged for 5 days, 10 days, 20 days, and 50 days. The growth behavior of the IMPs during the aging treatments was examined in the same way as mentioned above.

Transformation temperatures for the solder alloys were determined from heating curves obtained by differential scanning calorimetric (DSC) measurement at a heating rate of 5°C/min.

RESULTS AND DISCUSSION

Melting Behavior and As-Cast Microstructure of Zn-4Al and Zn-4Al-1Cu Alloys

Figure 2 shows the DSC heating curves for the Zn-4Al and Zn-4Al-1Cu specimens, where the first endothermic peaks appeared at 282°C and 285°C, caused by the monotectoid reaction of Al-rich face-centered cubic (fcc) + hexagonal close-packed (hcp) (Zn) = Zn-rich fcc, which is shown in the Zn-Al phase diagram in Fig. 1a. The second large endothermic peaks at 381°C and 380°C correspond to the eutectic melting reaction of Zn-rich fcc + hcp (Zn) = liquid. Figure 3 shows as-cast microstructures of these alloys. Both of them exhibit a hypoeutectic microstructure consisting of the primary crystal of hcp (Zn), Zn-rich fcc, and a eutectic lamellar structure. According to the EPMA analysis, the bright grains represents the hcp (Zn) (97.7 mass% Zn) and the dark particles with a complex microstructure represent the Zn-rich fcc

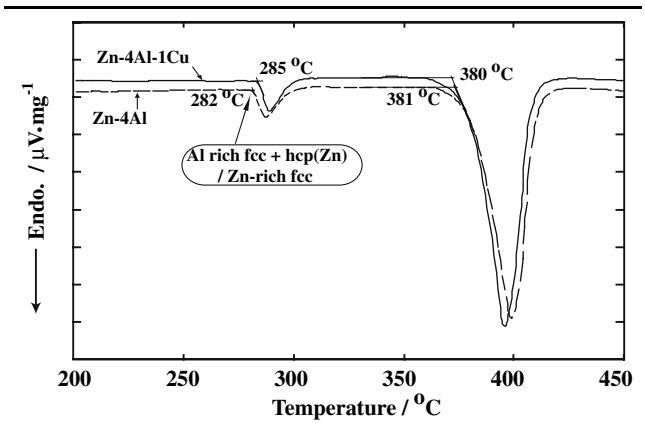

Fig. 2. Heating curves of DSC analysis measured in Zn-4Al and Zn-4Al-1Cu alloys.

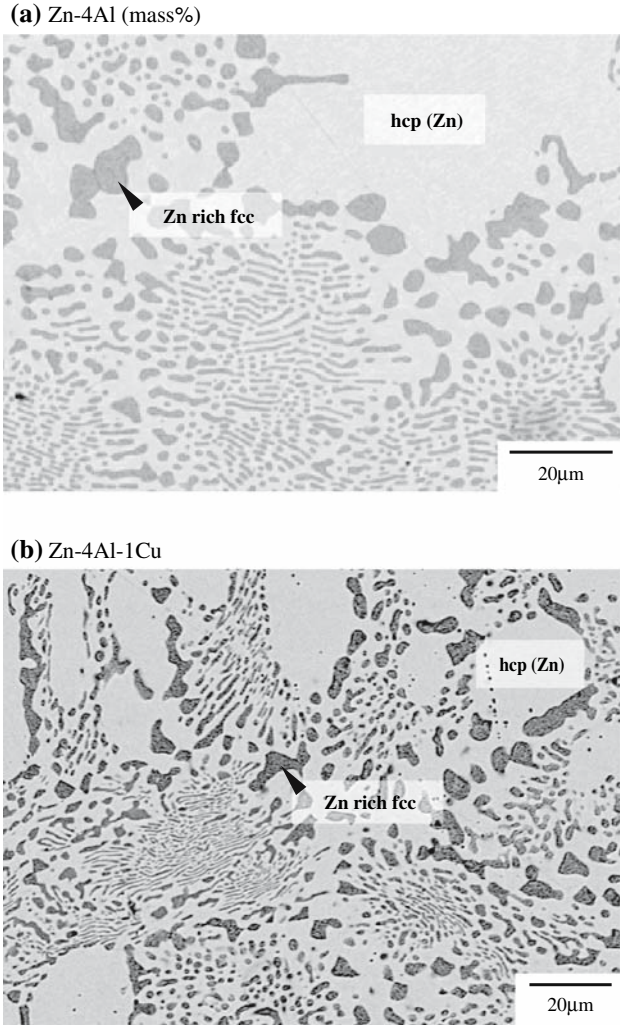

Fig. 3. Microstructure of (a) Zn-4Al and (b) Zn-4Al-1Cu as-cast alloys.

phase (83.1% Zn), which was decomposed into Al-rich fcc + hcp (Zn) by the monotectoid reaction during cooling. These results show that the addition of 1 mass%Cu to Zn-Al hardly influences the melting behaviors and the as-cast microstructure.

Consumption of the Cu Substrate During Soldering

During the soldering treatment, the Cu substrate is consumed by Zn and the formation and growth of the IMPs take place simultaneously at the soldered interface. Figure 4a shows the microstructure at the Cu/Zn-4Al-1Cu interface soldered at 450°C for 5 min. Two broken lines are superimposed on the optical micrograph; the upper one corresponds to the initial surface of the Cu substrate and the lower one indicates the front line of the phase interface between the Cu and β' phases. Here, it is noteworthy that the upper line corresponds to the Matano interface. The distance between these two lines, i.e., the migration distance of the Cu/$\beta(\beta')$ interface, is defined as the Cu consumption depth d, as shown in

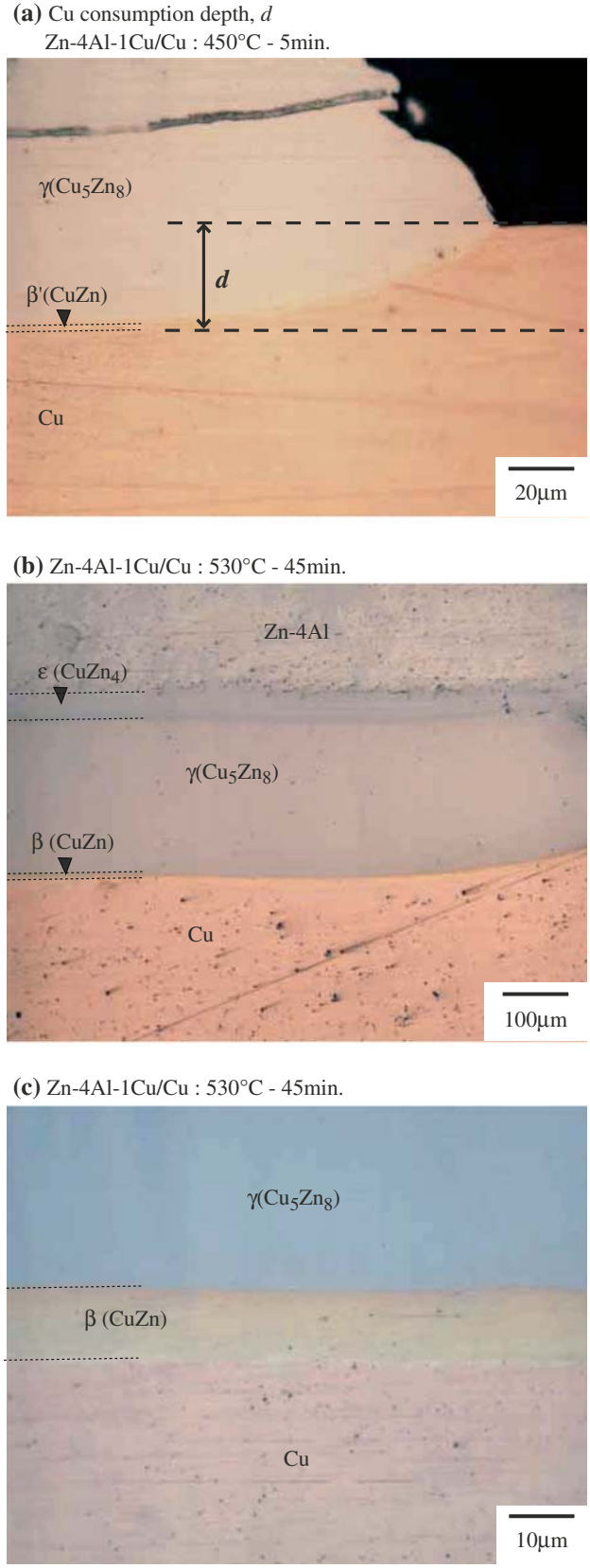

Fig. 4. Microstructures of Cu/molten Zn-4Al-1Cu (a) soldered at 450°C for 5 min showing consumption of the Cu substrate depth d, (b) soldered at 530°C for 45 min showing IMPs of ε, γ, and β, and (c) a magnified view of (b) near the interface of γ, β, and Cu.

Fig. 4a. Meanwhile, three IMPs, i.e., the ε, γ, and β phases form in the diffusion zone, as shown in Fig. 4b and c. Figure 5 shows the relationship between d and soldering time t for the Cu/Zn-4Al and Cu/Zn-4Al-1Cu assemblies soldered at temperatures between 420°C and 530°C, where d is plotted against the square root of t. Although it is known that metallic dissolution does not always follow a parabolic low, especially in the early stages,[6] a linear relationship obeying the parabolic law is confirmed in each specimen. The parabolic law is given by

$$d = k\sqrt{t}, \tag{1}$$

where k represents the coefficient for the consumption rate that corresponds to the slope of regression lines in Fig. 5a and b. The experimental values of k are listed in Table I. The rate coefficient for interface migration is described by an Arrhenius-type equation:

$$k = k_0 \exp\left(-\frac{Q}{RT}\right), \tag{2}$$

where k_0, Q, and R represent the migration rate constant, the activation energy, and the gas constant, respectively. Then, the values of k_0, and Q were evaluated from the Arrhenius plot of ln k against $1/T$ as shown in Fig. 6, where the slope and y-intercept of the regression lines correspond to $-Q/R$ and ln k_0, respectively. The values obtained are listed in Table I. Even though the differences of k_0 and Q between the two alloys are quite small, the suppressive effect of 1 mass% Cu in the Zn-4Al alloy on the consumption of the Cu substrate was confirmed. In the Sn-Ag-Cu Pb-free solder, Alam et al. have suggested that the addition of 0.5 mass% Cu to the Sn-3.5Ag solder results in a significant decrease in the consumption rate of the Cu substrate[7] due to the decrease of the concentration gradient of Cu in the Sn-3.5Ag solder. The decrease of the consumption rate in the Zn-4Al-1Cu solder may be analogous to their case.

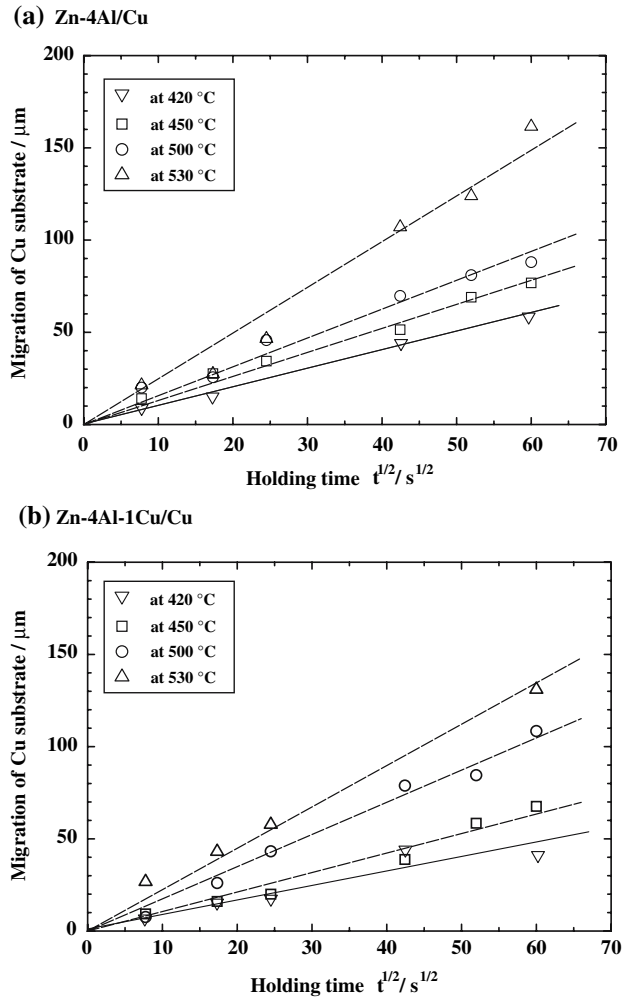

Fig. 5. The migration of Cu depth (d) evolutions of (a) Cu/molten Zn-4Al and (b) Cu/molten Zn-4Al-1Cu alloys.

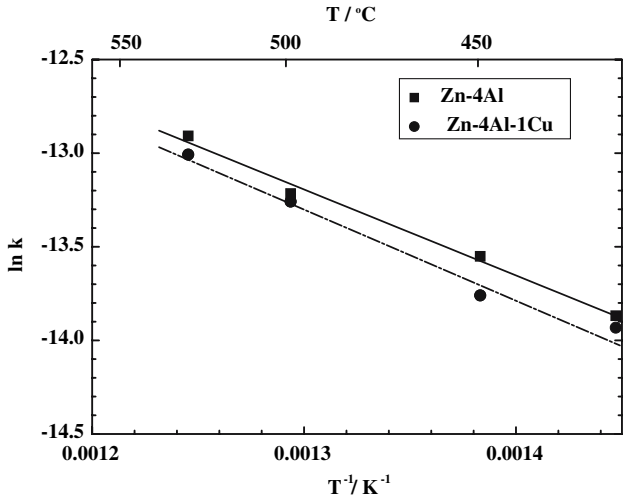

Fig. 6. Arrhenius plots of the migration rate coefficient of Cu substrate of Cu/molten Zn-Al base alloys.

Table I. Consumption Properties of the Cu Substrate During Soldering in Cu/Molten Zn-Al Base Alloys

Solder	k (m s$^{-1/2}$) 420°C	450°C	500°C	530°C	k_0 (m s$^{-1/2}$)	Activation Energy Q (kJ/mol)
Zn-4Al	9.21×10^{-7}	1.30×10^{-6}	1.56×10^{-6}	2.48×10^{-6}	9.49×10^{-4}	39.88
Zn-4Al-1Cu	8.88×10^{-7}	1.06×10^{-6}	1.75×10^{-6}	2.24×10^{-6}	8.87×10^{-4}	40.05

Growth of IMP Layers During Soldering

The soldering reaction between the molten Zn-Al base alloy and the Cu substrate results in the formation and growth of various IMPs as well as the consumption of the Cu substrate. Optical micrographs showing three kinds of IMP layers are exhibited in Fig. 4b and c. The thickness of each layer was measured along straight lines across all the interphase boundaries and the chemical composition of each IMP was determined by EPMA. Figure 7a and b shows the SEM-BSE image and the concentration-penetration profiles corresponding to the image, respectively, obtained from the Cu/Zn-4Al couple annealed at 420°C for 15 min. It can be seen that the initial interface is located at around the center of the IMP layer and that the liquid solder phases already include several mass percent of Cu. While the solder alloy includes 4 mass% Al, the interphase concentrations, which usually correspond to the equilibrium concentrations, seem to be consistent with the phase diagram in the Cu-Zn binary system as shown in Fig. 1b. On the other hand, it is seen that Al partitions to the β' phase more than to the ε phase.

Figure 8 shows the relationship between the thickness of the IMPs l and the soldering time t of

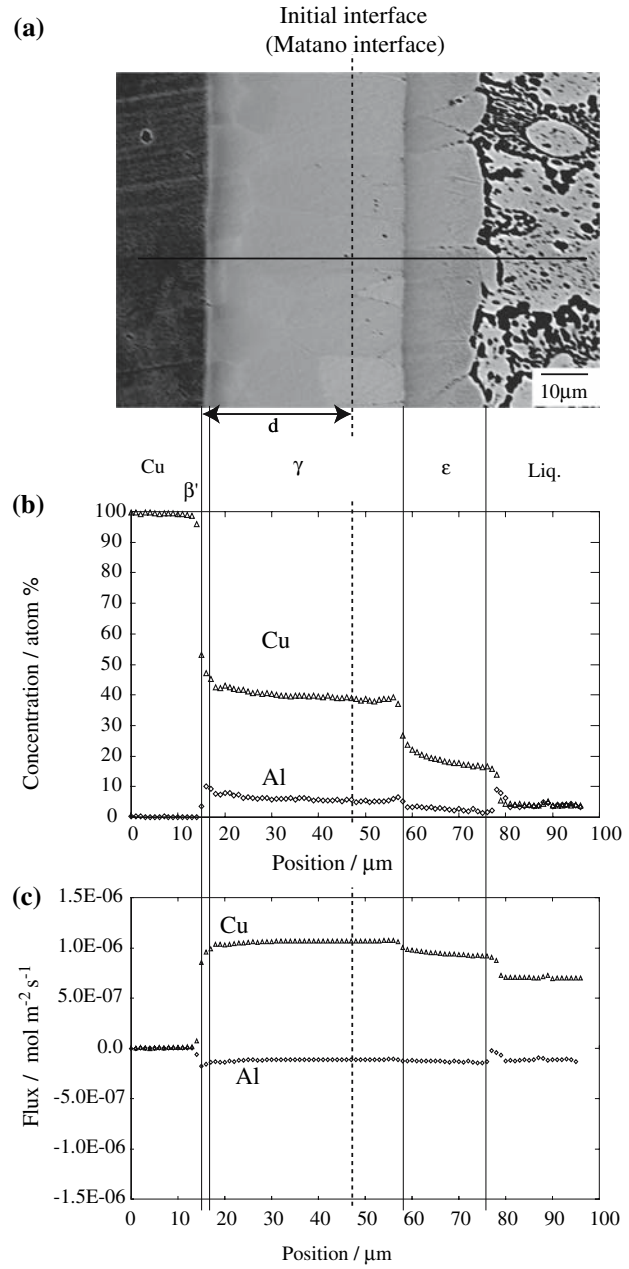

Fig. 7. (a) SEM-BSE image and (b) the concentration-penetration profiles corresponding to the image obtained from the Cu/Zn-4Al couple annealed at 420°C for 15 min. (c) Interdiffusion flux of Cu evaluated by Eq. 6 using the experimental concentration penetration profile.

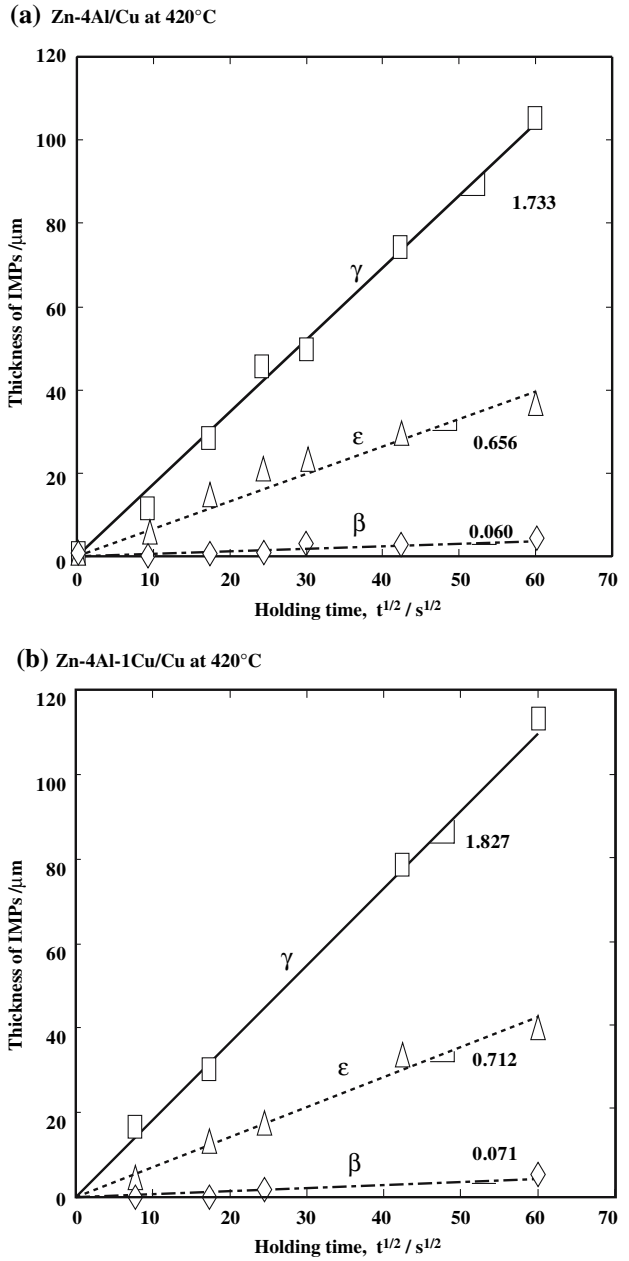

Fig. 8. Thickness evolutions of IMPs formed in (a) Cu/molten Zn-4Al and (b) Cu/molten Zn-4Al-1Cu soldered at 420°C.

Table II. Properties of IMPs Growth During Soldering in Cu/Molten Zn-Al Base Alloys

Solder	IMPs	k (m s$^{-1/2}$) 420°C	450°C	500°C	530°C	k_0 (m s$^{-1/2}$)	Activation Energy Q (kJ/mol)
Zn-4Al	β/β'(CuZn)	6.01×10^{-8}	6.58×10^{-8}	1.48×10^{-7}	2.70×10^{-7}	3.84×10^{-3}	64.73
	$\gamma(Cu_5Zn_8)$	1.73×10^{-6}	2.56×10^{-6}	3.56×10^{-6}	4.85×10^{-6}	2.27×10^{-3}	41.19
	$\varepsilon(CuZn_4)$	6.57×10^{-7}	9.72×10^{-7}	1.04×10^{-6}	1.12×10^{-6}	2.35×10^{-5}	20.02
Zn-4Al-1Cu	β/β'(CuZn)	7.10×10^{-8}	8.52×10^{-8}	2.56×10^{-7}	9.25×10^{-7}	3.02×10^{-3}	48.77
	$\gamma(Cu_5Zn_8)$	1.83×10^{-6}	2.56×10^{-6}	3.40×10^{-6}	9.47×10^{-6}	1.09×10^{-3}	36.69
	$\varepsilon(CuZn_4)$	7.12×10^{-7}	9.25×10^{-7}	9.47×10^{-6}	1.13×10^{-6}	1.32×10^{-5}	16.54

Cu/Zn-4Al and Cu/Zn-4Al-1Cu assemblies soldered at 420°C for durations between 1 min and 60 min. The linear relationship between l and the square root of t was confirmed, which suggests that the growth of IMPs is controlled by volume diffusion of the constituent elements and follows the parabolic law expressed by Eq. 1. In the growth of IMPs, the k in Eq. 1 represents the growth rate coefficient which was determined by the slope of the regression lines. The values of k for each experimental condition are summarized in Table II. The growth rate coefficient increases in the order of $k_{\beta/\beta'} < k_\varepsilon \ll k_\gamma$within the temperature range of this experimental work. In this table, the disordered β and ordered β' phase form at high temperature (500°C and 530°C) and at low temperature (420°C and 450°C), respectively.

The addition of 1 mass% Cu results in a decrease of the activation energy of the IMP growth and enhances the growth of the IMP layers. The preexisting Cu in the molten Zn-4Al solder seems to accelerate the formation and growth of the Cu-Zn IMPs. The overall reactions during soldering at 420°C, i.e., the consumption of the Cu substrate and the formation and growth of IMPs, are summarized quantitatively in Fig. 9. The relative positions of the Cu/IMP and liquid/IMP interfaces are located below and above the initial interface, respectively. The width between these two curves corresponds to the total thickness (L) of the three IMP layers. Both the consumption rate of the Cu substrate and the growth of the IMP in the Cu/Zn-Al base alloys are higher than those of Cu/Sn base solders.[8]

The Arrhenius plots of the IMP growth during soldering are shown in Fig. 10. The growth rate constant k_0 and the activation energy Q evaluated

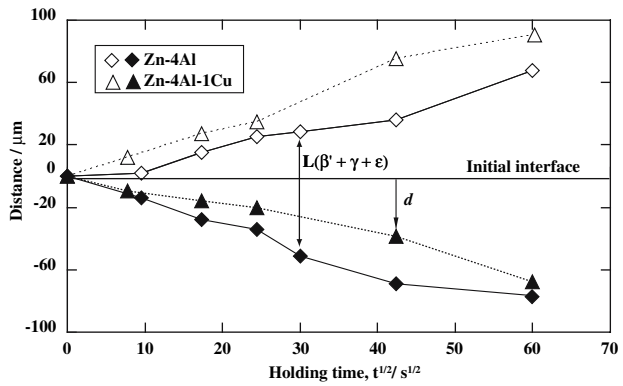

Fig. 9. Average migration of Cu (d) and total IMP thickness (L) between the Cu and molten Zn-Al base solders at 420°C.

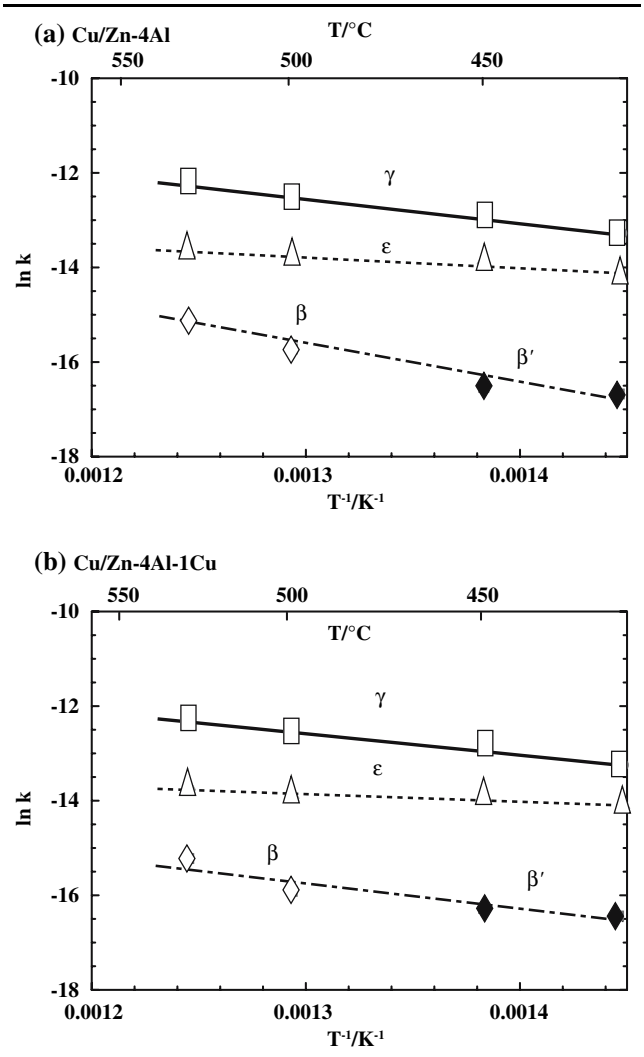

Fig. 10. Arrhenius plots of the growth rate coefficient of IMPs, ε, γ, and β'/β formed in Cu/Zn-Al base alloys during soldering.

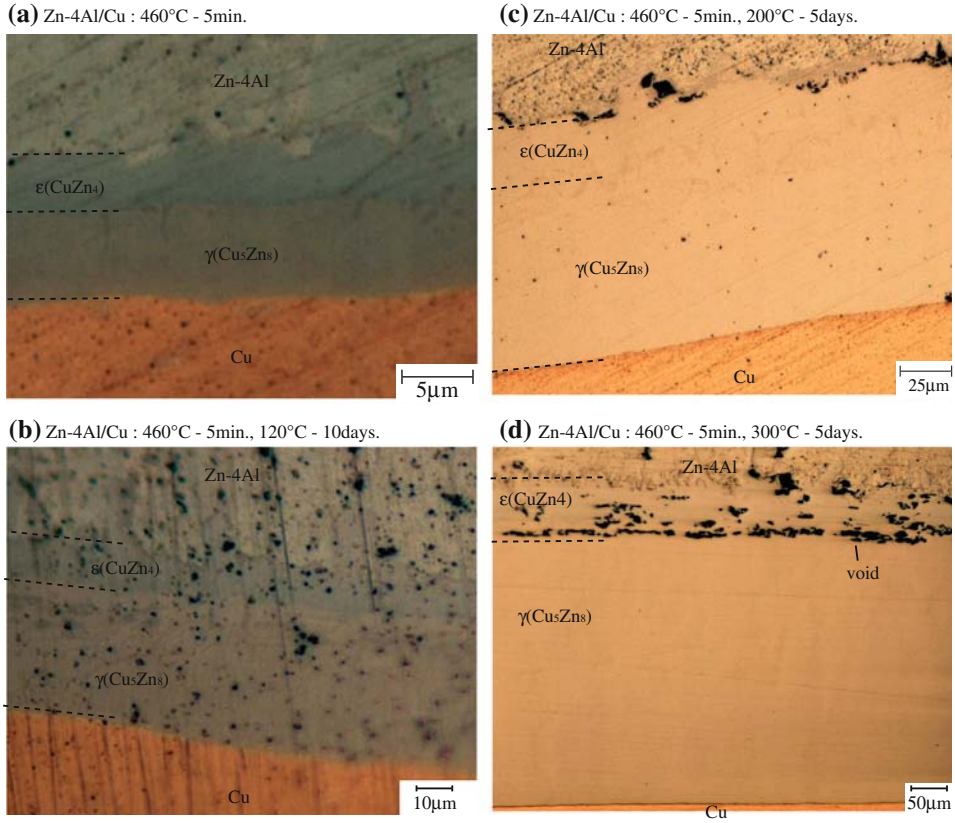

Fig. 11. Microstructures of (a) Cu/molten Zn-4Al soldered at 460°C for 5 min, and Cu/IMPs/solid Zn-4Al aged at (b) 120°C for 10 days, (c) 200°C for 5 days, and (d) 300°C for 5 days after the soldering treatment.

from the Arrhenius plots are summarized in Table II. It is seen that, even though the activation energy decreases in the order $Q_\varepsilon < Q_\gamma < Q_\beta$, the growth rate coefficient increases in the order $k_\beta < k_\varepsilon < k_\gamma$ within the temperature range of this experimental work.

Let us explain the behaviors of the growth rate and the activation energy of the IMPs. According to Fick's first law, the interdiffusion flux in the binary system is given by

$$\tilde{J} = -\tilde{D}\frac{\partial c}{\partial x}, \tag{3}$$

where $\tilde{D}$ and $\partial c/\partial x$ are the interdiffusion coefficient and the concentration gradient of profile, respectively. If the concentration range, Δc^i, of the intermediate phase i is small and the concentration profile in its phase region is almost straight, Eq. 3 is approximately given by

$$\tilde{J} \approx -\tilde{D}_i\frac{\Delta c^i}{\Delta x^i}, \tag{4}$$

where Δx^i is the width of the i phase layer and $\tilde{D}_i$ is the interdiffusion coefficient of the i phase. Consequently, Δx^i can be simply estimated by

$$\Delta x^i \approx -\frac{\tilde{D}_i \cdot \Delta c^i}{\tilde{J}}, \tag{5}$$

This relation means that the layer thickness of an IMP is proportional to the interdiffusion coefficient and the concentration range of the IMP. According to the Boltzmann–Matano analysis, the interdiffusion flux for a concentration c_1 in the concentration profile is obtained using the experimental profile by

$$\tilde{J} = \frac{1}{2t}\int_{c0}^{c1} x\,\mathrm{d}c, \tag{6}$$

where c_0 is the composition of a master alloy. This analysis is not applicable to the determination of the flux for the liquid phase in the solid-liquid diffusion couple because of the convection flow of the solute element in the liquid phase. However, when the diffusion condition is steady for the whole duration of diffusion and the position of the Matano interface is known, the flux of the solid phases can be estimated by Eq. 6. Figure 7c shows the interdiffusion flux of Cu evaluated by this equation using the experimental concentration penetration profile for the Cu/Zn-4Al couple, where the position of the initial interface is used as the Matano interface and the pure Cu is the master alloy with c_0 in Eq. 3. Here, it should be noted that the atomic flux data determined for the liquid phase after 80 μm show a low accuracy because a chemical segregation in solidification occurs during cooling. It is seen that the Cu fluxes of all the IMPs are not so different and

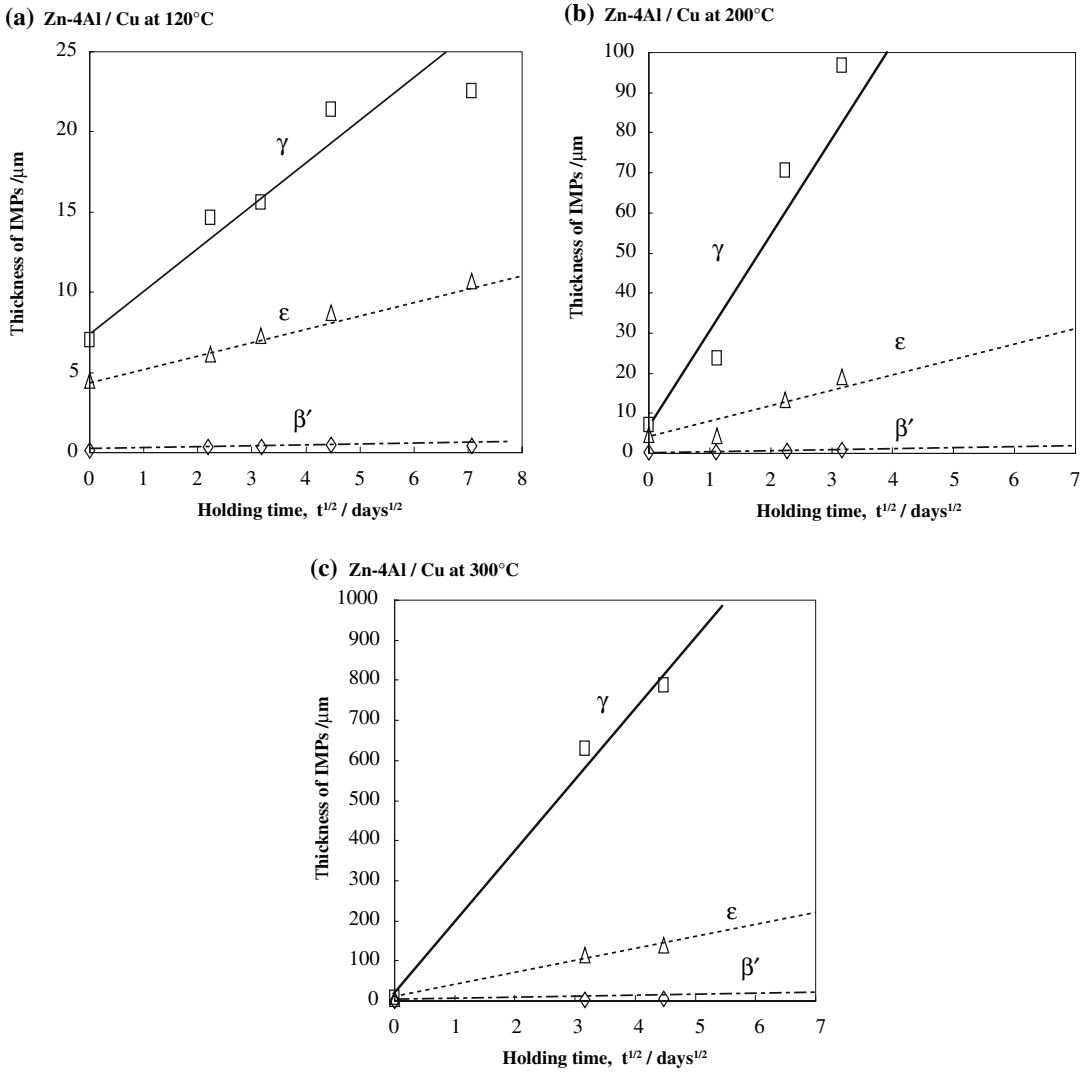

Fig. 12. Thickness evolutions of IMPs formed in Cu/solid Zn-4Al at 460°C for 5 min and aging at (a) 120°C, (b) 200°C, and (c) 300°C.

are located in the region between 8.5 and 11×10^{-7} mol m^{-2} s^{-1}. From the Zn-Cu phase diagram in Fig. 1b, the solubility concentration range Δc^{γ} and Δc^{ε} for the γ and ε phases are about 10 mass% at 420°C, while Δc^{β} for the β phase is several percent. On the other hand, the $\tilde{D}$ of each IMP in the Zn-Cu alloys has already been reported as $\tilde{D}_{\beta'} = 10^{-14}-10^{-13}$ (m^2/s),[9] $\tilde{D}_{\gamma} = 10^{-12}-10^{-11}$ (m^2/s),[10] $\tilde{D}_{\varepsilon} = 10^{-13}-10^{-12}$ (m^2/s)[11] between 380°C and 450°C, being in the order of $\beta' < \varepsilon < \gamma$. It can be concluded from Eq. 5 that the difference in the growth rate for the IMPs shown in Fig. 8 is mainly due to the differences of both the interdiffusivity and the solubility range among them.

As shown in Fig. 10 and Table II, the activation energies for the growth of the IMPs are in the order $Q_{\varepsilon} < Q_{\gamma} < Q_{\beta}$. Since the activation energies for diffusion should be in the order $\gamma < \varepsilon < \beta$ from the relation of interdiffusivity mentioned above, a different order, i.e., $Q_{\gamma} < Q_{\varepsilon} < Q_{\beta}$, is expected for the growth of the IMPs. This discrepancy may be due to the difference in the temperature dependence of the solubility concentration range. According to the Zn-Cu phase diagram, Δc^{γ} slightly increases with increasing temperature, while Δc^{β} and Δc^{ε} drastically increase and decrease, respectively. This change influences the temperature dependence of the growth rate constant; i.e., in the β phase, Δc^{β} is widened with increasing temperature, Δx^{β} is enhanced at elevated temperatures and Q_{β} becomes high, while in the ε phase Δc^{ε} is decreased, Δx^{ε} is reduced at elevated temperatures and Q_{β} becomes low, as deduced from Eq. 5.

Growth of IMP Layers During Aging

Cu/Zn-4Al and Cu/Zn-4Al-1Cu assemblies soldered at 460°C for 5 min were heated again at 120°C, 200°C, and 300°C and aged for 5–50 days. Then the further growth of IMP layers which formed during the soldering treatment was

Table III. Properties of IMPs Growth During Aging in Cu/Solid Zn-Al Base Alloys

Solder	IMPs	k (m s$^{-1/2}$) 120°C	200°C	300°C	k_0 (m s$^{-1/2}$)	Activation Energy Q (kJ/mol)
Zn-4Al	β'(CuZn)	2.37×10^{-10}	7.64×10^{-10}	2.90×10^{-9}	–	–
	γ(Cu_5Zn_8)	8.74×10^{-9}	9.32×10^{-8}	6.20×10^{-7}	7.08×10^{-3}	44.37
	ε($CuZn_4$)	3.00×10^{-9}	1.37×10^{-8}	1.08×10^{-7}	2.23×10^{-4}	37.06
Zn-4Al-1Cu	β'(CuZn)	9.47×10^{-10}	1.21×10^{-9}	2.03×10^{-9}	–	–
	γ(Cu_5Zn_8)	9.47×10^{-9}	1.37×10^{-7}	3.90×10^{-7}	1.80×10^{-3}	39.03
	ε($CuZn_4$)	6.35×10^{-9}	3.60×10^{-8}	1.17×10^{-7}	7.35×10^{-5}	30.40

observed. Figure 11 shows the microstructure in the vicinity of the diffusion zone of the Cu/Zn-4Al couple: (a) as-soldered, (b) aged at 120°C for 10 days, (c) aged at 200°C for 5 days, and (d) aged at 300°C for 5 days. The initial thickness of each IMP layer, d_0, should be taken into account. Then, Eq. 1 should be modified as

$$d = d_0 + k\sqrt{t}, \tag{7}$$

where d, d_0, k, and t represent the average thickness of IMPs, the initial thickness, the growth rate coefficient, and the aging duration, respectively. Figure 12 shows the growth of IMPs layers of Cu/Zn-4Al aged at (a) 120°C, (b) 200°C, and (c) 300°C, where the β' phase layer is too thin to be qualitatively evaluated based on the SEM-BSE image and the data obtained for the β' thickness seems to contain considerable uncertainty. The linear relationship between the layer thickness d and the holding time t was confirmed, which suggests that each growth of the IMPs is controlled by volume diffusion of the constituent elements and follows the parabolic law expressed by Eq. 7. The results for Cu/Zn-4Al-1Cu are basically comparable to those for Cu/Zn-4Al. The values of k determined for all the specimens are summarized in Table III. It is seen that the growth rate coefficient increases in the order $k_{\beta'} < k_\varepsilon \ll k_\gamma$ within the temperature range of this experimental work. In particular, the rates of the growth of the γ and ε layer in the Cu/Zn-Al base alloys are higher than those of Cu/Sn base solders.[12,13] During aging over 4 days at 200°C, the layer thickness of the γ phase exceeds 50 μm, which reaches the width of the solder layer between the Si-chip and Cu substrate. Thus in this type of Cu/Zn-Al(-Cu) assembly special attention to the growth behavior of the γ layer is required.

Furthermore, during aging treatment at higher temperatures and for longer durations, the formation of a considerable number of voids was observed. The voids formed mainly at the interface in the Zn-Al(-Cu) alloy when the samples were aged at 200°C and inside the ε phase aged at 300°C as shown in Fig. 11c and d. The formation of voids during aging is clearly brought about by the Kirkendall effect due to the difference of diffusivity between Cu and Zn, which may cause detachment and loss of reliability of the solder joint.

CONCLUSIONS

Interfacial reactions between Cu/Zn-4Al and Cu/Zn-4Al-1Cu with regard to the consumption of the Cu substrate, and the growth of the IMPs during soldering and aging treatments were investigated. The consumption of the Cu substrate and the growth of IMPs during soldering were found to be controlled by the volume diffusion of constituent elements. The formation and growth of some intermediate phases (IMPs) such as β(A2: disordered bcc) or β'(B2:ordered bcc), γ($D8_2$: Cu_5Zn_8) and ε(A3: disordered hcp) were observed, and the activation energy increased in the order $Q_\varepsilon < Q_\gamma < Q_\beta$, which is explained by diffusivity and the solubility concentration range from Zn-Cu phase diagram. In view of the aging process, the growth of IMPs is considered to be controlled by the volume diffusion. In particular, the layer thickness of γ rapidly grows over 200°C, although the thickness of β layer grows quite slowly.

With the addition of 1 mass% Cu in Zn-4Al solder, the suppression of the consumption of Cu substrate was confirmed. This resulted in the decrease of the activation energy of the IMP growth and enhanced the growth of the IMP layers, particularly the Cu-Zn IMPs.

ACKNOWLEDGEMENT

Support from CREST, the Japan Science and Technology Agency, is acknowledged.

REFERENCE

1. G. Matijasevic, C. Wang, and C. Lee, *IEEE Trans. Comp. Hybrids Manuf. Technol.* 13(4), 1128 (1990).
2. T. Shimizu, H. Ishikawa, I. Ohnuma, and K. Ishida, *J. Electron. Mater.* 28, 1172 (1999).
3. H. Okamoto, *J. Phase Equilib.* 16(3), 281 (1995).
4. M. Rettenmayer, P. Lambrancht, B. Kenpf, and C. Tschudin, *J. Electron. Mater.* 31, 278 (2002).
5. A.P. Miodownink, *Phase Diagrams of Binary Copper Alloy*, ed. P.R. Subramanian and D.E. Laughlin (Materials Park, OH: ASM International, 1994), pp. 487–496.
6. E.S. Machliin, *An Introduction to Aspects of Thermodynamics and Kinetics Relevant to Materials Science* (Giro Press, 1991), pp. 278–286.

7. M.O. Alam, Y.C. Chan, and K.N. Tu, *J. Appl. Phys.* 94, 7904 (2003).
8. Y. Takaku, X.J. Liu, I. Ohnuma, R. Kainuma, and K. Ishida, *Mater. Trans.* 45, 646 (2004).
9. Y. Funamizu and K. Watanabe, *J. Jpn. Inst. Met.* 39, 1087 (1975).
10. Yu.E. Ugaste, *Fiz. Met. Metalloved.* 27, 663 (1969).
11. Y. Funamizu and K. Watanabe, *Trans. Jpn. Inst. Met.* 17, 59 (1976).
12. P.T. Vianco, J.A. Rejent, and P.F. Hlava, *J. Electron. Mater.* 33, 991 (2004).
13. J.W. Yoon and S.B. Jung, *J. Mater. Sci.* 39, 4211 (2004).